

The first hyperpolarizability of *p*-nitroaniline in 1,4-dioxane: A quantum mechanical/molecular mechanics study

Lasse Jensen^{a)}

Department of Chemistry, Northwestern University, Evanston, Illinois 60208-3113

Piet Th. van Duijnen

Theoretical Chemistry, Materials Science Centre, Rijksuniversiteit Groningen, Nijenborgh 4, 9747 AG Groningen, The Netherlands

(Received 23 May 2005; accepted 14 June 2005; published online 22 August 2005)

In this work we have investigated the first hyperpolarizability of *p*NA in 1,4-dioxane solution using a quantum mechanics/molecular mechanics (QM/MM) model. The particular model adopted is the recently developed discrete solvent reaction field (DRF) model. The DRF model is a polarizable QM/MM model in which the QM part is treated using time-dependent density-functional theory and local-field effects are incorporated. This allows for direct computation of molecular effective properties which can be compared with experimental results. The solvation shift for the first hyperpolarizability is calculated to be 30% which is in good agreement with the experimental results. However, the calculated values, both in the gas phase and in solution, are by a factor of 2 larger than the experimental ones. This is in contrast to the calculation of the first hyperpolarizability for several small molecules in the gas phase where fair agreement is found with experimental. The inclusion of local-field effects in the calculations was found to be crucial and neglecting them led to results which are significantly larger. To test the DRF model the refractive index of liquid 1,4-dioxane was also calculated and found to be in good agreement with experiment.

© 2005 American Institute of Physics. [DOI: 10.1063/1.1999633]

I. INTRODUCTION

Understanding the linear and nonlinear optical (NLO) properties of materials is an important research area. Materials exhibiting NLO effects are of great technological importance for use in future application within electronics and photonics.^{1,2} The second-harmonic generation (SHG) is of particular interest and many studies have been devoted to the investigation of this property. The SHG properties of organic molecules are characterized in terms of their molecular first hyperpolarizability, $\beta(-2\omega; \omega, \omega)$, which can be measured using electric-field-induced second-harmonic generation³⁻⁵ (EFISH) or hyper-rayleigh scattering^{6,7} (HRS) techniques. These experiments are usually performed in solution.

Typical organic chromophores which are of interest are the so-called push-pull or donor-accepter molecules due to their large value for the first hyperpolarizability.^{1,8} The prototype push-pull molecule is *para*-nitroaniline (*p*-NA) and there exist in the literature many studies of its first hyperpolarizability both theoretically and experimentally. However, due to different conventions it is often difficult to compare results obtained in different experiments and calculations. For a clear discussion about this, the reader is referred to the work by Willetts *et al.*⁹

In a recent study of the first hyperpolarizability,

$$\beta_{||} = \frac{1}{5} \sum_{\alpha} \beta_{z\alpha\alpha} + \beta_{\alpha z\alpha} + \beta_{\alpha\alpha z}, \quad (1)$$

of *p*-NA in different solvents using HRS calibrated against carbon tetrachloride,¹⁰ in 1,4-dioxane solution a $\beta_{||}=1482$ a.u. at 1064 nm was reported, using the *T* convention.⁹ The *T* convention refers to expanding the induced dipole moment in a Taylor series, and will be used throughout this paper. It should be mentioned that in the HRS measurements the high symmetry of *p*-NA in combination with an assumption of a rodlike molecule has been used to extract individual tensor components.⁹ This result is in good agreement with EFISH results provided the standard reference for quartz is taken to be $d_{11}=0.30$ pm/V at 1064 nm.¹⁰ This reference is believed to be more accurate than the older value of 0.5 pm/V.¹¹⁻¹³ The EFISH values are $\beta_{||}=1359$ a.u. (Ref. 14) and $\beta_{||}=1409$ a.u. (Ref. 15) both corrected to comply with the new reference value and the *T* convention.¹⁶ Note that it has been argued that the convention in the original EFISH experiments^{14,15} was the *B** convention, which would make the results larger by a factor of 3.⁹ However, the good agreement between the EFISH and HRS measurements reported in Ref. 10 contradicts this.

The first hyperpolarizability of *p*-NA has been found experimentally to depend strongly on the solvent both in the EFISH and the HRS methods.^{6,10,14,17} Theoretically, a similar strong dependence has been found using a continuum solvation model.¹⁸ The strong solvent dependence is usually described in terms of a two-state model.^{14,17-20} Recently, an experimental study found for solvents not forming H bonds a

^{a)} Author to whom correspondence should be addressed. Electronic mail: l.jensen@chem.northwestern.edu

good linear correlation of the form $\beta = \beta_{\text{gas}} + a\sqrt{\mu_s/V_s}$ where, μ_s is the dipole moment of the solvent in the gas phase, V_s the molar volume in the liquid state, and β_{gas} is considered to be the first hyperpolarizability in the gas phase.¹⁷ The references used in the measurements were the first hyperpolarizability of *p*-NA in 1,4-dioxane at 1064 nm adopted from Ref. 15. They reported a value in the gas phase to be $\beta_{\parallel} = 1008$ a.u., here corrected for differences in reference value and conventions.¹⁶ This value is in good agreement with the value of $\beta_{\parallel} = 1072 \pm 44$ a.u. for *p*NA measured in the gas phase.²¹

The difference in β_{\parallel} of *p*-NA in the gas phase and in 1,4-dioxane solution is therefore only around 30%. Theory predicts a slightly larger increase due to solvation, around 50% using the self-consistent reaction field model¹⁸ and around 43% using the nonequilibrium version of the model.²² There has also been a discrete quantum-mechanical Langevin dipoles/Monte Carlo study of β_{\parallel} of *p*-NA in water and chloroform solutions.²³ For the chloroform solution an increase by almost a factor of 2 is reported. Although they did not study 1,4-dioxane solution the experiments show that the results in the two solutions are almost identical.^{10,14}

In this work we will study β_{\parallel} of *p*-NA in 1,4-dioxane using a recent developed quantum mechanics/molecular mechanics (QM/MM) model.²⁴⁻²⁷ This discrete solvent reaction field model (DRF) combines a time-dependent density-functional theory (TD-DFT) description of the solute molecule with a classical (MM) description of the discrete solvent molecules. The latter are represented by distributed atomic charges and polarizabilities. The model has recently been extended to enable the calculation of both microscopic (hyper)polarizabilities and macroscopic (non)linear susceptibilities.^{27,28} Although the first hyperpolarizability of *p*-NA in 1,4-dioxane has been studied before this is the first investigation using a QM/MM model.

II. THE DISCRETE SOLVENT REACTION FIELD MODEL

In the DRF model the QM/MM operator at a point r_i is given by²⁴⁻²⁷

$$\begin{aligned} \hat{H}_{\text{QM/MM}} &= \sum_i v^{\text{DRF}}(r_i, \omega) = \sum_i v^{\text{el}}(r_i) + \sum_i v^{\text{pol}}(r_i, \omega) \\ &= \sum_{i,s} \frac{q_s}{R_{si}} + \sum_{i,s} \mu_{s,\alpha}^{\text{ind}}(\omega) \frac{R_{si,\alpha}}{R_{si}^3}, \end{aligned} \quad (2)$$

where the first term v^{el} is the electrostatic operator and describes the Coulombic interaction between the QM system (the solute) and the permanent charge distribution of the solvent molecules. The second term v^{pol} is the polarization operator which describes the many-body polarization of the solvent molecules, i.e., the change in the permanent charge distribution of the solvent molecules due to interaction with the QM part and other solvent molecules. The charge distribution of the solvent is represented by atomic point charges and the many-body polarization term is represented by induced atomic dipoles at the solvent molecules.

The induced atomic dipole at a site s is given by

$$\mu_{s,\alpha}^{\text{ind}}(\omega) = \alpha_{s,\alpha\beta} \left[F_{s,\beta}^{\text{init}}(\omega) + \sum_{t \neq s} T_{st,\beta\gamma}^{(2)} \mu_{t,\gamma}^{\text{ind}}(\omega) \right], \quad (3)$$

where $\alpha_{s,\alpha\beta} = \delta_{\alpha\beta} \alpha_s$ is a component of the polarizability tensor of an isotropic atom at site s , and $T_{st,\alpha\beta}^{(2)}$ is the screened dipole interaction tensor.^{24,29,30} We assume that the atomic polarizabilities are independent of the frequency, but the model can easily be extended to include also this effect.^{31,32}

$F_{s,\beta}^{\text{init}}(\omega)$ is the initial electric field at site s and consists of four terms

$$F_{s,\beta}^{\text{init}}(\omega) = F_{s,\beta}^{\text{QM,el}}(\omega) + F_{s,\beta}^{\text{QM,nuc}} + F_{s,\beta}^{\text{MM,q}} + F_{s,\beta}^{\text{mac}}(\omega), \quad (4)$$

where $F_{s,\beta}^{\text{QM,el}}(\omega)$ is the field arising from the frequency-dependent electronic charge distribution of the QM part, $F_{s,\beta}^{\text{QM,nuc}}$ is the field from the QM nuclei, $F_{s,\beta}^{\text{MM,q}}$ is the field from the point charges at the solvent molecules, and $F_{s,\beta}^{\text{mac}}(\omega)$ is the macroscopic electric field. The inclusion of the macroscopic electric field in Eq. (3) gives rise to additional dipole moments induced in the solvent.^{27,28}

The DRF operator is combined with the time-dependent Kohn-Sham equations,³³⁻³⁷

$$i \frac{\partial}{\partial t} \phi_i(r, t) = \left[-\frac{1}{2} \nabla^2 + v_{\text{eff}}(r, t) \right] \phi_i(r, t), \quad (5)$$

where the effective potential is given by

$$v_{\text{eff}}(r, t) = \int dr' \frac{\rho(r', t)}{|r - r'|} + v^{\text{per}}(t) + v^{\text{DRF}}(r, t) + v_{\text{xc}}(r, t), \quad (6)$$

with $v^{\text{DRF}}(r, t)$ the operator defined in Eq. (2) and $v^{\text{per}}(t)$ the potential of the macroscopic perturbing field. The last term is the time-dependent xc potential adopted in the adiabatic local-density approximation (ALDA). The time-dependent electronic density is then given by

$$\rho(r, t) = \sum_i^{\text{occ}} n_i |\phi_i(r, t)|^2, \quad (7)$$

where n_i is the occupation number of orbital i . The (hyper) polarizabilities can be found using response theory in combination with the finite field method.^{25,26}

We have shown²⁷ that this approach enables the calculation of different microscopic properties including different solvent effects. The first effect is due to the interaction between the solute and the solvent (pure solvent effect) and is calculated with the macroscopic electric field *not included* in Eq. (4). The microscopic properties calculated in this way will be denoted as “solute properties.” If the macroscopic electric field is *included* in Eq. (4) we will denote the calculated properties as “effective.” The effective properties include, in addition to the pure solvent effect, the influence of the dipole moments induced in the solvent by the macroscopic electric field. We showed^{27,28} that these are effective properties that have to be combined with the Lorentz local-field factors¹ to describe the macroscopic susceptibilities.

III. COMPUTATIONAL DETAILS

The DRF model has been implemented into a local version of the AMSTERDAM DENSITY-FUNCTIONAL (ADF) program package^{38,39} by an extension to the TD-DFT part in the RESPONSE module of ADF.^{40–42} The details of the implementation are described in Refs. 24–27.

All structures used in this work have been optimized with the Becke-Perdew xc functional^{43,44} and the TZ2P basis set. Except for water where the structure was taken from Ref. 27. The response calculations were done using the gradient-regulated asymptotic connection Becke-Perdew (BP-GRAC) potentials.^{45,46} The BP-GRAC potential sets the highest occupied molecular orbital (HOMO) level at the first ionization potential (IP) and therefore requires the IP as input. The values for IP were obtained from calculations using the statistical average of model orbital potentials (SAOP) for which it has been shown that the HOMO level corresponds well with the experimental IP.⁴⁷

The molecular-dynamics (MD) simulations were performed with the discrete reaction field polarizable force field^{30,48–52} using the DRF90 program.⁴⁸ A MD simulation of 50 ps with a time step of 1 fs was performed at 298 K, using a Nose-Hoover thermostat⁵³ (with $\tau=1$ ps) to keep the temperature constant and a soft wall force potential⁴⁸ to keep the particles inside the simulation box. After every 0.5 ps, the configuration of solvent molecules was kept. This gives a total of 100 configurations for which QM/MM calculations were performed. Although the total number of configurations is somewhat small it should still give an accurate average since the configurations are uncorrelated.⁵⁴

Two simulations were performed, one for pure 1,4-dioxane and one for *p*-NA in 1,4-dioxane, each simulation having 1 solute and 100 solvent molecules placed in a spherical box with a radius of 34 bohr. The sizes of the simulation boxes were chosen so that the simulated macroscopic densities correspond to the experimental value of 1.0337 kg/l for 1,4-dioxane. In the simulations, the molecules were treated as rigid bodies using quaternions.⁵⁵ For *p*-NA and 1,4-dioxane multipole derived charge analysis (MDC)-*d* charges were used⁵⁶ that were obtained from DFT calculations in a TZ2P basis set with the ADF program. The standard DRF90 potential was used in the simulations.⁴⁸ Standard atomic polarizabilities³⁰ were used for 1,4-dioxane whereas for *p*-NA atomic polarizabilities were fitted to reproduce the polarizability calculated using ADF. The atomic polarizability parameters for *p*-NA are $\alpha_C=13.4187$, $\alpha_H=0.6207$, $\alpha_O=3.1970$, and $\alpha_N=17.4651$ a.u.

IV. RESULTS

A. The first hyperpolarizability of selected molecules in the gas phase

There has been a recent study in which the first hyperpolarizability of a series of small molecules has been measured in the gas phase using the EFISH method and calibrated against the second hyperpolarizability of N₂.²¹ Adopting the same series of molecules in this work will provide a very good benchmark for the DFT calculation performed in this work. We have therefore performed DFT

TABLE I. Gas phase properties of selected molecules. Dipole moments in Debye and first hyperpolarizability in a.u. The experimental results is from Ref. 21. The frequency is $\omega=0.0428$ a.u.

Molecule	Method	μ	$\beta_{ }(-2\omega; \omega, \omega)$	ρ_{N_2}/ρ_X
CHCl ₃	DFT	1.01	-4.3	9.1
CDCl ₃	Expt.	1.04	1.0±4	8.0
CH ₃ CN	DFT	3.99	16.00	4.0
	Expt.	3.92	17.9±1.1	3.8
CH ₃ OH	DFT	1.60	-43.13	2.6
CH ₃ OD	Expt.	1.70	-31.2±1.6	2.6
CH ₃ NO ₂	DFT	3.43	-45.8	4.8
CD ₃ NO ₂	Expt.	3.46	-33.7±1.5	5.4
H ₂ O	DFT	1.80	-20.6	1.3
	Expt.	1.85	-19.2±0.9	1.4
C ₆ H ₅ NO ₂ ^a	DFT	4.55	435.9	31.5
	Expt.	4.22	197±9	24.1
<i>p</i> -NA	DFT	7.73	2127.3	88.3
	Expt.	6.87	1072±44	42.4

^aNitrobenzene (NB).

calculations of the dipole moment, frequency-dependent polarizability, and first hyperpolarizability at $\omega=0.0428$ a.u. ($\lambda=1064$ nm). The dipole moments and first hyperpolarizabilities have been collected in Table I and compared with the experimental results. The EFISH experiments have been performed using periodic phase matching conditions to insure maximum signal.^{57–59} Problems with phase matching in the experiments arise from the dispersion in the refractive index of the sample and phase matching conditions can be achieved simply by varying the density of the sample. The phase-match densities are related to the refractive index, which is proportional to the polarizability well below any resonance, and the ratio between the reference N₂ and the sample X is given by^{57–59}

$$\rho_{N_2}/\rho_X = \frac{\bar{\alpha}^X(2\omega) - \bar{\alpha}^X(\omega)}{\bar{\alpha}^{N_2}(2\omega) - \bar{\alpha}^{N_2}(\omega)}. \quad (8)$$

In Table I we also present the ratio of the phase match densities (ρ_{N_2}/ρ_X) for N₂ gas and the sample vapor. If the ratio of the phase match densities is wrong the measured first hyperpolarizability could be wrong by the same factor.⁶⁰

For the dipole moments we find in general a very good agreement between the experimental values and the results calculated using DFT. The only exception is *p*-NA for which the DFT result is larger by about 15%. The gas phase value reported for the dipole moment of *p*-NA in Ref. 21 is a theoretical MP2 result.⁶¹ For the first hyperpolarizability we find excellent agreement for the molecules CHCl₃, CH₃CN, and H₂O whereas for CH₃OH and CH₃NO₂ the DFT absolute values are larger by 38% and 35%, respectively. For nitrobenzene (NB) and *p*-NA the differences is even larger. The DFT values are larger by a factor of 2.2 and 2.0 for NB and *p*-NA, respectively. If we now consider the phase-match densities we see that for all molecules but NB and *p*-NA there is a good agreement between theory and experiment.

TABLE II. Static and frequency-dependent properties of 1,4-dioxane in gas phase and liquid phase. Dipole moments in Debye and the polarizability and first hyperpolarizability in a.u. The frequency is $\omega=0.0428$ a.u. The solute and effective properties are reported as the average value \pm the standard error. The standard error is given by σ/\sqrt{N} where σ is the standard deviation and N is the number of configurations.

	μ	$\bar{\alpha}(-0;0)$	$\bar{\alpha}(-\omega;\omega)$	$\bar{\alpha}(-2\omega;2\omega)$	$\bar{\beta}(-0;0,0)$	$\bar{\beta}(-2\omega;\omega,\omega)$
Vacuum	0.009D	58.79	59.24	60.69	-0.38	-0.47
Solute	0.05 \pm 0.04	62.89 \pm 0.04	63.39 \pm 0.04	64.96 \pm 0.04	1.18 \pm 2.27	1.10 \pm 2.68
Effective	0.05 \pm 0.04	58.47 \pm 0.06	58.92 \pm 0.06	60.37 \pm 0.07	3.90 \pm 2.30	4.39 \pm 2.66

For NB the calculated phase-match ratio is larger than the measured ratio by 30% and for *p*-NA the calculated ratio is larger by a factor of 2. If we “correct” the experimental results according to the differences in the phase-match ratio we get a first hyperpolarizability of $\beta_{II}=257$ a.u. and $\beta_{II}=2232.5$ a.u. for NB and *p*-NA, respectively. This brings the experimental results for *p*-NA in good agreement with the theoretical results obtained here. However, the result for NB is still calculated to be larger than the experiments by around 70%. A recent comparison of DFT and CC hyperpolarizabilities by Salek *et al.*⁶² reported for *p*-NA at $\omega=0.0428$ a.u. values of $\beta_{II}=1579.3$ a.u. and $\beta_{II}=1797.3$ a.u. using CCSD and DFT-B3LYP, respectively, here again corrected for differences in conventions.¹⁶ Both of these results are significant larger than the experimental results, although the CCSD results are closer to the measured values than the DFT results. In these calculations only a medium-sized basis set (Sadlej basis for DFT and a stripped down aug-cc-pVTZ basis for CCSD) was used whereas in this work a very large basis set with many diffuse functions was used. The differences in the basis sets could account for some of the discrepancy in the theoretical results. Salek *et al.* also found that the dispersion of β_{II} was overestimated by DFT as compared to CCSD.⁶² The larger dispersion would also cause the phase densities to be overestimated. It is therefore quite likely that some of the differences between the calculated and measured phase-match densities are simply due to the larger dispersion. The results obtained by Salek *et al.* was claimed to be in good agreement with the experiments, however, the “good” agreement came from comparing the results obtained in different conventions and in fact their results are larger than the experiments by around 50% for CCSD and 70% for DFT. In this work we have adopted perfect planar structures for both NB and *p*-NA. It is well known that conformational changes in these structures greatly affects the molecular properties.^{63–65} The first hyperpolarizability of *p*-NA has its maximum for the planar structure and rotating the amino group results in a lowering of the first hyperpolarizability.^{63–65} Some of the discrepancy between theory and experiments could be explained if the experimental structure, in fact, is nonplanar.

B. The refractive index of 1,4-dioxane

Before discussing the results for *p*-NA in 1,4-dioxane, which is the main focus of this work, we will discuss the results obtained for pure 1,4-dioxane. This will allow us to verify the solvent model used in the *p*-NA calculations. The

gas phase properties and in solution both the solute and effective properties for 1,4-dioxane are collected in Table II.

The ground-state structure of 1,4-dioxane has a C_{2h} symmetry with a chair conformation for the ring. In this work the structure adopted has the slightly lower symmetry of C_s but still in the chair conformations. This will be unimportant for the main results presented here, however, the structure will have a small dipole moment and first hyperpolarizability due to the lower symmetry. From Table II we see that both the dipole moment and first hyperpolarizability in the gas phase are indeed small. We also see that the solute properties are not very different from the gas phase properties, i.e., the pure solvent effects are rather small. In solution we see that the dipole moment is slightly larger but still very small. The first hyperpolarizability is increased too in going to the liquid phase, especially the effective values. However, in all cases the standard error is of the same order as the mean and therefore to obtain a better average more configurations would be needed. For the polarizability we see that α^{sol} is increased compared with the gas phase and that α^{eff} is almost identical to the gas phase value although slightly lower. The difference between the solute and effective properties is due to the screening of the electric field by the dipole moments induced in the liquid.^{27,28} We see that the standard error for the polarizability is much smaller than the mean values.

The linear refractive index (or the optical dielectric constant) of the system is related to the linear susceptibility and is given by^{27,28}

$$n^{(1)}(\omega_s) = \sqrt{\epsilon^{(1)}(\omega_s)} = \sqrt{1 + 4\pi\chi_{ZZ}^{(1)}(-\omega_s; \omega_s)}$$

$$= \sqrt{\frac{1 + (8\pi/3)N_d\bar{\alpha}^{\text{eff}}(-\omega_s; \omega_s)}{1 - (4\pi/3)N_d\bar{\alpha}^{\text{eff}}(-\omega_s; \omega_s)}}, \quad (9)$$

which is the familiar Lorentz-Lorenz or Clausius-Mossotti equation,^{66–68} with the effective polarizability instead of the gas phase polarizability. We can therefore use the polarizabilities reported in Table II to calculate the refractive index of liquid 1,4-dioxane. The results are listed in Table III and compared with experimental results. We see that there is a fair agreement between the calculated and measured refractive indices. The calculated refractive index is slightly larger

TABLE III. Refractive index of liquid 1,4-dioxane at $\omega=0.0428$ a.u.

	$n(\omega)$	$n(2\omega)$
DFT	1.430	1.442
Expt. ^a	1.416	1.426

^aRefractive index from Ref. 74.

TABLE IV. Static and frequency-dependent properties of *p*-NA in gas phase and 1,4-dioxane solution. Dipole moments in Debye and the polarizability and first hyperpolarizability in a.u. The frequency is $\omega=0.0428$ a.u. The solute and effective properties are reported as the average value \pm the standard error. The standard error is given by σ/\sqrt{N} where σ is the standard deviation and N is the number of configurations.

	μ	$\bar{\alpha}(-0;0)$	$\bar{\alpha}(-\omega;\omega)$	$\bar{\alpha}(-2\omega;2\omega)$	$\bar{\beta}(-0;0,0)$	$\bar{\beta}(-2\omega;\omega,\omega)$
Vacuum	7.73D	110.31	113.57	128.85	978.21	2127.3
Solute	10.62 \pm 0.06	128.80 \pm 0.16	134.44 \pm 0.19	166.90 \pm 0.49	1841.92 \pm 7.13	4625.00 \pm 25.40
Effective	10.62 \pm 0.06	115.81 \pm 0.18	120.61 \pm 0.33	148.17 \pm 0.47	1108.00 \pm 9.74	2770.99 \pm 26.48

than the experimental results which was also found previously for other liquids using the DRF model.²⁷ This is most likely due to the fact that DFT predicts larger polarizabilities in the gas phase than, e.g., CCSD.^{27,62} The good agreement with the calculated and measured refractive indices for pure 1,4-dioxane validates that the solvent model adopted is adequate.

C. The first hyperpolarizability of *p*-NA in 1,4-dioxane

Having verified the solvent model we continue with the main objective of this study which is to calculate the first hyperpolarizability of *p*-NA in 1,4-dioxane. The gas phase, solute and effective solution phase properties of *p*-NA are presented in Table IV. All calculations were done for $\omega = 0.0428$ a.u. A typical example of one of the configurations used in the QM/MM calculations is displayed in Fig. 1. From the table it is clear that there is a strong pure solvent effect on the properties of *p*-NA, i.e., the solute properties are significantly enhanced relative to the gas phase results. The dipole moment μ^{sol} is increased by 37% which is a much larger increase than the previously found using a self-consistent reaction field model.¹⁸ A recent experiment estimates the dipole moment for *p*-NA in benzene to be 7.6 D.⁶⁹ Although the solvents are different it indicates that this di-

pole moment in solution is smaller than what we find. It should be noted that the dipole moment of a molecule in solution is not a quantity which can be measured and is typically extracted from the dielectric constant. Also the dipole moment of *p*-NA in the gas phase calculated in this work is much larger than the value obtained with MP2.⁶¹

The polarizability at frequencies 0, ω , and 2ω increases by 17%, 18%, and 30%, respectively. This means that the dispersion of the polarizability is enhanced in solution. The solvent effect on the first hyperpolarizability is much larger: it is increased by 88% and 117% for the static and frequency-dependent β^{sol} , respectively. Similar large enhancements were found in earlier theoretical studies.^{18,22,23} For the effective properties we again see the lowering of the properties due to the screening field arising from the dipoles in the solvent induced by the macroscopic electric field. In the effective polarizability at frequencies 0, ω , and 2ω the increase is now 5%, 6%, and 15%, respectively. The lowering of β^{eff} compared with β^{sol} is much larger and the increase compared with the gas phase is only 13% and 30% for the static and frequency-dependent first hyperpolarizabilities, respectively. The inclusion of the macroscopic electric field in Eq. (4) is therefore crucial for obtaining results which can be compared with experimental values. The first hyperpolarizability in 100 different QM/MM configurations is presented in Fig. 2. From the figure it is clear that β^{sol} is significantly larger than β^{eff} which is enhanced somewhat compared to the gas phase value. It also illustrates the large fluctuations among the different configurations, both for the effective and solute first hyperpolarizabilities.

As discussed in the Introduction, experimental values for $\beta_{\parallel} = 1482$ a.u. using HRS and $\beta_{\parallel} = 1359$ a.u. (Ref. 14) and $\beta_{\parallel} = 1409$ a.u. (Ref. 15) using EFISH were reported for *p*-NA in 1,4-dioxane. We calculated $\beta_{\parallel}^{\text{eff}} = 2770.99$ a.u. which is larger than the experimental result by a factor of 2. This was also what was found in the gas phase. Therefore, if we instead compare solvation shifts, i.e., $\beta^{\text{solvent}}/\beta^{\text{gas}}$, we find good agreement between theory and experiment since both predict a 30% increase.

V. DISCUSSION

The accurate prediction of NLO properties of molecules requires large basis sets, high-level electron correlation, frequency-dependence, and both electronic and vibrational contributions to be included.⁷⁰ Even in the gas phase this is only feasible for small molecules due to the high computational demands, see Refs. 71–73 for examples. There all contributions were included systematically and therefore good

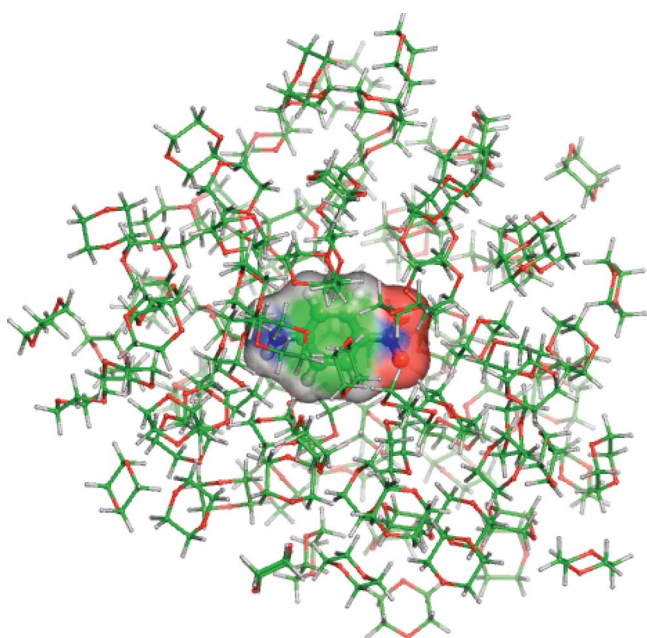


FIG. 1. (Color) A typical configuration of *p*-NA in a 1,4-dioxane cluster used in the QM/MM calculations. The *p*-NA molecules has been highlighted with a surface. The figure has been made using PYMOL Ref. 75.

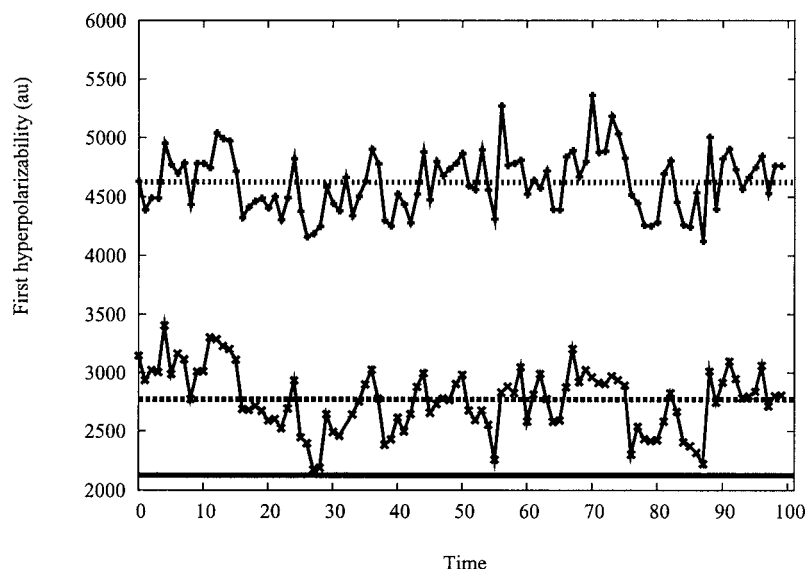


FIG. 2. The first hyperpolarizability of *p*-NA in gas phase and in 1,4-dioxane solution for the 100 QM/MM configurations. Top line is for β^{sol} , the middle line for β^{eff} , and the bottom line is the gas phase value for β .

agreement with experiments was found. The prerequisite for validating calculated results is the availability of accurate experimental results for the molecule in the gas phase. The experimental EFISH results by Kaatz *et al.*²¹ for the molecules listed in Table I is a good example of this and should make a reliable benchmark for comparison with accurate theoretical results. We did such a preliminary benchmark comparison for the DFT method adopted in this work. In some cases the agreement was very good while in others, and especially for *p*-NA, the agreement was quite disappointing. We therefore suggest a more systematic comparison at a higher level of theory than DFT, e.g., CCSD or even CCSD(T). This should include also the dipole moment and second hyperpolarizability since both of these are required to extract the first hyperpolarizability in the EFISH experiment. This will then also give a reliable theoretical benchmark for comparison with different DFT methods. However, as mentioned above some of the discrepancy between theory and experiments for *p*-NA could be due to the assumption that *p*-NA is close to being planar. Calculating β_{\parallel} by averaging over many different *p*-NA configurations should be done to investigate the importance of nonplanarity of the molecule. If this indeed is the case perhaps *p*-NA should not be considered as a good reference point for comparing theory and experiments.

In the condensed phase the situation is even more difficult due to complications when extracting microscopic properties from the measured macroscopic properties. We have shown that by including local-field effects in a QM/MM description it is possible to directly calculate the effective properties which can be compared with experimental results using the standard Lorentz/Onsage local-field theory.^{27,28} However, the model is limited by the accuracy obtained in the gas phase. If we compare the shift in the first hyperpolarizability due to solvation we find good agreement between theory and experiments. We do find that the solvent effect in a nonpolar solvent, such as 1,4-dioxane, is fairly modest. It would therefore be interesting to repeat this study using different solvents to see if the solvation shifts found experimentally can be reproduced.

VI. CONCLUSIONS

We have calculated the first hyperpolarizability of *p*-NA in 1,4-dioxane solution using a quantum mechanics/molecular mechanics (QM/MM) model. We adopted the discrete solvent reaction field (DRF) model which we recently have developed. The DRF model is a polarizable QM/MM model where the QM part is treated using time-dependent density-functional theory (TD-DFT) and local-field effects have been incorporated leading to molecular effective properties which can be compared with experimental results. The TD-DFT model was first tested by calculating the first hyperpolarizability of several small molecules in the gas phase and compared these results with experimental results. In some cases the agreement was very good while in others, and especially for *p*-NA, the agreement was quite disappointing. For *p*-NA the results were off by a factor of 2. Several different possible explanations for the discrepancy were discussed. To test the solvent model the refractive index of liquid 1,4-dioxane was calculated and found to be in good agreement with the experimental results. For the calculation of the first hyperpolarizability in solution the inclusion of the local-field factors was found to be crucial. The calculated solvation shift for the first hyperpolarizability was found to be 30% which is in good agreement with the experimental results. However, the calculated values for the first hyperpolarizability is larger than the experiments by a factor of 2, i.e., about the same factor as in the gas phase. Further investigations are suggested to resolve some of the discrepancy between theory and experiments both in gas phase and in solution.

¹P. N. Prasad and D. J. Williams, *Introduction to Nonlinear Optical Effects in Molecules and Polymers* (Wiley, New York, 1991).

²*Molecular Electronics*, edited by J. Jortner and M. Ratner (Blackwell Science, Oxford, 1997).

³B. F. Levine and C. G. Bethea, *J. Chem. Phys.* **63**, 2666 (1975).

⁴J. L. Oudar and D. S. Chemla, *J. Chem. Phys.* **66**, 2664 (1977).

⁵K. D. Singer and A. F. Garito, *J. Chem. Phys.* **75**, 3572 (1981).

⁶K. Clays and A. Persoons, *Phys. Rev. Lett.* **66**, 2980 (1991).

⁷E. Hendrickx, K. Clays, and A. Persoons, *Acc. Chem. Res.* **31**, 675 (1998).

- ⁸D. R. Kanis, M. A. Ratner, and T. J. Marks, *Chem. Rev. (Washington, D.C.)* **94**, 195 (1994).
- ⁹A. Willetts, J. E. Rice, D. M. Burland, and D. Shelton, *J. Chem. Phys.* **97**, 7590 (1992).
- ¹⁰P. Kaatz and D. P. Shelton, *J. Chem. Phys.* **105**, 3918 (1996).
- ¹¹I. Shoji, T. Kondo, and R. Ito, *Opt. Quantum Electron.* **34**, 797 (2002).
- ¹²U. Gubler and C. Bosshard, *Phys. Rev. B* **61**, 10702 (2000).
- ¹³C. Bosshard, U. Gubler, P. Snd Kaatz, W. Mazerant, and U. Meier, *Phys. Rev. B* **61**, 10688 (2000).
- ¹⁴M. Stählin, D. M. Burland, and J. E. Rice, *Chem. Phys. Lett.* **191**, 245 (1992).
- ¹⁵C. C. Teng and A. F. Garito, *Phys. Rev. B* **28**, 6766 (1983).
- ¹⁶The conversion factor is: $\beta_{||} = (0.3/0.5) \times 2 \times 3/5 \times \beta$, where the first factor corrects for the reference value, the second factor corrects for difference conventions (*T* vs *B*) and the last factor is the relation between $\beta_{||}$ and β . 1 a.u. = 8.6392×10^{-33} esu.
- ¹⁷F. L. Huyskens, P. L. Huyskens, and A. P. Persoons, *J. Chem. Phys.* **108**, 8161 (1998).
- ¹⁸K. V. Mikkelsen, Y. Luo, H. Ågren, and P. Jørgensen, *J. Chem. Phys.* **100**, 8240 (1994).
- ¹⁹J. N. Woodford, M. A. Pauley, and C. H. Wang, *J. Phys. Chem. A* **101**, 1989 (1997).
- ²⁰C.-K. Wang, Y.-H. Wang, Y. Su, and Y. Luo, *J. Chem. Phys.* **119**, 4409 (2003).
- ²¹P. Kaatz, E. A. Donley, and D. P. Shelton, *J. Chem. Phys.* **108**, 849 (1998).
- ²²P. Norman, Y. Luo, D. Jonsson, H. Ågren, K. O. Sylvester-Hvid, and K. V. Mikkelsen, *J. Chem. Phys.* **107**, 9063 (1997).
- ²³W. Bartkowiak, R. Zalesny, W. Niewodniczański, and J. Leszczynski, *J. Phys. Chem. A* **105**, 10702 (2001).
- ²⁴L. Jensen, P. T. van Duijnen, and J. G. Snijders, *J. Chem. Phys.* **118**, 514 (2003).
- ²⁵L. Jensen, P. T. van Duijnen, and J. G. Snijders, *J. Chem. Phys.* **119**, 3800 (2003).
- ²⁶L. Jensen, P. T. van Duijnen, and J. G. Snijders, *J. Chem. Phys.* **119**, 12998 (2003).
- ²⁷L. Jensen, M. Swart, and P. T. van Duijnen, *J. Chem. Phys.* **122**, 034103 (2005).
- ²⁸L. Jensen and P. T. van Duijnen, *Int. J. Quantum Chem.* **102**, 612 (2005).
- ²⁹B. T. Thole, *Chem. Phys.* **59**, 341 (1981).
- ³⁰P. T. van Duijnen and M. Swart, *J. Phys. Chem. A* **102**, 2399 (1998).
- ³¹L. Jensen, P.-O. Åstrand, K. O. Sylvester-Hvid, and K. V. Mikkelsen, *J. Phys. Chem. A* **104**, 1563 (2000).
- ³²L. Jensen, P.-O. Åstrand, A. Osted, J. Kongsted, and K. V. Mikkelsen, *J. Chem. Phys.* **116**, 4001 (2002).
- ³³E. Runge and E. K. U. Gross, *Phys. Rev. Lett.* **52**, 997 (1984).
- ³⁴E. K. U. Gross and W. Kohn, *Adv. Quantum Chem.* **21**, 255 (1990).
- ³⁵R. van Leeuwen, *Int. J. Mod. Phys. B* **15**, 1969 (2001).
- ³⁶M. E. Casida, in *Recent Advances in Density-Functional Methods*, edited by D. P. Chong (World Scientific, Singapore, 1995), p. 155.
- ³⁷M. E. Casida, in *Recent Developments and Applications of Modern Density Functional Theory*, edited by J. M. Seminario (Elsevier, Amsterdam, 1996).
- ³⁸G. te Velde, F. M. Bickelhaupt, E. J. Baerends, C. Fonseca Guerra, S. J. A. van Gisbergen, J. G. Snijders, and T. Ziegler, *J. Comput. Chem.* **22**, 931 (2001).
- ³⁹ADF, <http://www.scm.com> (2005).
- ⁴⁰S. J. A. van Gisbergen, J. G. Snijders, and E. J. Baerends, *Comput. Phys. Commun.* **118**, 119 (1999).
- ⁴¹S. J. A. van Gisbergen, J. G. Snijders, and E. J. Baerends, *J. Chem. Phys.* **103**, 9347 (1995).
- ⁴²S. J. A. van Gisbergen, J. G. Snijders, and E. J. Baerends, *J. Chem. Phys.* **109**, 10644 (1998).
- ⁴³A. D. Becke, *Phys. Rev. A* **38**, 3098 (1988).
- ⁴⁴J. P. Perdew, *Phys. Rev. B* **33**, 8822 (1986).
- ⁴⁵M. Grüning, O. V. Gritsenko, S. J. A. van Gisbergen, and E. J. Baerends, *J. Chem. Phys.* **114**, 652 (2001).
- ⁴⁶M. Grüning, O. V. Gritsenko, S. J. A. van Gisbergen, and E. J. Baerends, *J. Chem. Phys.* **116**, 9591 (2002).
- ⁴⁷D. P. Chong, O. V. Gritsenko, and E. J. Baerends, *J. Chem. Phys.* **116**, 1760 (2002).
- ⁴⁸M. Swart and P. T. van Duijnen, *Mol. Simul.* (to be published).
- ⁴⁹A. H. de Vries, P. T. van Duijnen, A. H. Juffer, J. A. C. Rullmann, J. P. Dijkman, H. Merenga, and B. T. Thole, *J. Comput. Chem.* **16**, 37 (1995).
- ⁵⁰A. H. de Vries, P. T. van Duijnen, R. W. Zijlstra, and M. Swart, *J. Electron Spectrosc. Relat. Phenom.* **86**, 49 (1997).
- ⁵¹P. T. van Duijnen and A. H. de Vries, *Int. J. Quantum Chem.* **60**, 1111 (1996).
- ⁵²P. T. van Duijnen, F. C. Grozema, and M. Swart, *J. Mol. Struct.: THEOCHEM* **464**, 193 (1999).
- ⁵³S. Toxvaerd, *Mol. Phys.* **72**, 159 (1991).
- ⁵⁴K. Coutinho, M. J. De Oliveira, and S. Canuto, *Int. J. Quantum Chem.* **66**, 249 (1998).
- ⁵⁵M. P. Allen and D. J. Tildesley, *Computer Simulations of Liquids* (Clarendon, Oxford, 1987).
- ⁵⁶M. Swart, P. T. van Duijnen, and J. G. Snijders, *J. Comput. Chem.* **22**, 79 (2001).
- ⁵⁷D. P. Shelton and A. D. Buckingham, *Phys. Rev. A* **26**, 2787 (1982).
- ⁵⁸D. P. Shelton and V. Mizrahi, *Phys. Rev. A* **33**, 72 (1986).
- ⁵⁹D. P. Shelton, *Phys. Rev. A* **42**, 2578 (1990).
- ⁶⁰D. P. Shelton (private communication).
- ⁶¹F. Sim, S. Chin, M. Dupuis, and J. E. Rice, *J. Phys. Chem.* **97**, 1158 (1993).
- ⁶²P. Salek, T. Helgaker, O. Vahtras, H. Ågren, D. Jonsson, and J. Gauss, *Mol. Phys.* **103**, 439 (2005).
- ⁶³G. J. M. Velders, J.-M. Gillet, P. J. Becker, and D. Feil, *J. Phys. Chem.* **95**, 8601 (1991).
- ⁶⁴G. J. M. Velders and D. Feil, *J. Phys. Chem.* **96**, 10725 (1992).
- ⁶⁵S. Yamada, K. Yamaguchi, K. Kamada, and K. Ohta, *Mol. Phys.* **101**, 309 (2003).
- ⁶⁶C. J. F. Böttcher, *Theory of Electric Polarization*, 2nd ed. (Elsevier, Amsterdam, 1973), Vol. 1.
- ⁶⁷J. D. Jackson, *Classical Electrodynamics*, 2nd ed. (Wiley, New York, 1975).
- ⁶⁸H. A. Lorentz, *The Theory of Electrons*, 1st ed. (B. G. Teubner, Leipzig, 1909).
- ⁶⁹E. M. Breitung, W. E. Vaughan, and R. J. McMahon, *Rev. Sci. Instrum.* **71**, 224 (2000).
- ⁷⁰D. M. Bishop, *Adv. Quantum Chem.* **25**, 1 (1994).
- ⁷¹C. Hättig and P. Jørgensen, *J. Chem. Phys.* **109**, 2762 (1998).
- ⁷²D. M. Bishop, F. L. Gu, and S. M. Cybulski, *J. Chem. Phys.* **109**, 8407 (1998).
- ⁷³H. Reis, M. G. Papadopoulos, and A. Avramopoulos, *J. Phys. Chem. A* **107**, 3907 (2003).
- ⁷⁴C. S. Liu, R. Glaser, P. Sharp, and J. F. Kauffman, *J. Phys. Chem. A* **101**, 7176 (1997).
- ⁷⁵W. L. Delano, *The PyMOL Molecular Graphics System*, <http://www.pymol.org> (2002).